



Targeted suppression of vibration in deep hole drilling using magneto-rheological fluid damper

Lingfei Kong^{a,*}, Jih-Hua Chin^b, Yan Li^a, Yanjun Lu^a, Pengyang Li^a

^a School of Mechanical and Instrumental Engineering, Xi'an University of Technology, Xi'an 710048, Shaanxi, PR China

^b Department of Mechanical Engineering, National Chiao Tung University, Hsinchu, Taiwan, ROC



ARTICLE INFO

Article history:

Received 7 November 2013

Received in revised form 24 May 2014

Accepted 26 May 2014

Available online 2 June 2014

Keywords:

Deep hole drilling

MR fluid vibration damper

Drilling tools system

Vibration suppression

ABSTRACT

Under the concept of precision or targeted vibration suppression, a novel approach is developed to reduce the vibration of drilling tool system in deep-hole drilling process. The concept is to suppress the dominant vibration upon its emergence by variable damping or to force the harmful vibration morph into less harmful by different damper position. A magneto-rheological (MR) fluid damper is designed with adjustable damping capability to counteract emerging vibration. A series of experimental investigations are carried out on the BTA deep hole drilling process. The experimental results show that the adjustable MR damping brings down the vibration in all applications with different suppression effect. A relative optimal suppression can always be found. The suppressed vibration experiences a frequency shift which sheds light on the possible avoidance of matching of unwelcome frequency. Different damper locations have different but consistent suppression results which foresee a possibility of forcing the mode of vibration into less harmful one. A potential precision or targeted suppression of vibration upon its emergence is thus possible.

© 2014 Elsevier B.V. All rights reserved.

1. Introduction

Deep hole drilling is one of the most value-adding manufacturing processes. Compared with the traditional drilling, deep hole drilling produces holes with good surface finish and straightness when the ratio of hole-depth to hole-diameter exceeds ten. However, owing to the length of tool shaft and its special design, i.e., the drill head is flushed by high pressure liquid, the process is susceptible to dynamic disturbances, chatter (Gessesse et al., 1994) and spiraling (Weinert et al., 2002) are among them. There have been investigations in the past decades leading to better understanding of deep hole drilling process; however, the desire of an effective means which allows a target-oriented stabilization of the process in the face of disturbance is still open.

There are two kinds of disturbances in deep hole drilling, one is of resonant nature and the other is of regenerative nature (Deng and Chin, 2004). Regeneration vibrations known as chatter is due to the interaction of the cutting force and the work-piece surface undulations produced by preceding tool passes. Over the last two decades, there has been an increased research effort to investigate chatter vibration and its suppression method in deep hole drilling process.

Bayly et al. (2002) studied the cutting and rubbing forces in a chisel drilling edge in addition to tool vibration, which produces an error in the hole size or “roundness error” of the drilled piece. Litak (2002) investigated theoretically the nonlinear interaction between the tool and a work-piece that leads to chatter vibrations of periodic, quasi-periodic or chaotic type, and analyzed the impact between the tool and a work-piece after their contact loss. Hussien et al. (2007) developed a mathematical approach to study the whirling motion of a continuous boring bar-workpiece system with internal cutting forces and external suppression forces by transforming the problem into nonhomogeneous equations with homogenous boundary conditions. Experimental results indicated that external suppression forces reduced the whirl amplitude at the same locations. Mehrabadi et al. (2009) investigated chatter vibration occurring in drills for deep hole machining, and proposed a numerical method to simulate the tool path at different radial widths of cut and spindle speeds. The numerical results show that even if chatter does not occur, spindle speed selection also affects roundness, concentricity, and surface roughness.

For chatter detection, Weinert et al. (2002) used dynamical systems to model the drilling process. They are interested in a local description of adequate accuracy to predict disturbances and to provide insights into their prevention. Therefore, they proposed a phenomenological approach with a special emphasis on the temporal neighborhoods of instabilities or state transitions from stable

* Corresponding author. Tel.: +86 18629322811.

E-mail addresses: lingfeikong@xaut.edu.cn, lingfei.kong@163.com (L. Kong).

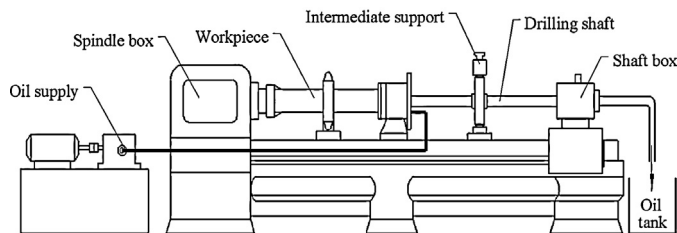


Fig. 1. Configuration of deep hole drilling machine.

drilling to chatter vibration and back. [Messaoud and Weihs \(2009\)](#) proposed a phenomenological model based on the Van Der Pol equation and used nonlinear time series to set up an on-line modeling of the time varying dynamics process. [Keraita et al. \(2001\)](#) proposed the acoustic emission method to investigate the instability of cutting or chatter by detecting AE signal parameters. Moreover, [Mei et al. \(2009\)](#) was the first to apply the MR fluid on chatter suppression in boring process, and further, a chatter recognition method was demonstrated that the composed of wavelet transform and SVM has an excellent performance for chatter premonition identification ([Yao et al., 2011](#)).

Deflections of resonant nature are investigated in depth by [Deng and Chin \(2004\)](#). It was found that the deflections brought about by modal shape weigh differently. Lower modal deflections tend to be more influential and are more responsible for vibration induced degradation of hole quality. This leads to the idea of precision or targeted suppression of unwelcome vibrations. A way to suppress the harmful vibrations or force them into less harmful vibrations is desirable. Such a vibration suppression would be meaningful in diminishing or curbing both resonant vibration and chatter. The purpose of this paper is therefore to propose the concept of targeted suppression of vibration and to design a device to implement the idea for BTA deep hole drilling.

A novel design and construction of MR fluid damper is developed. The “targeting” ability of this MR fluid damper arises from its possible variation of location of application and its variable damping capability. The influence of the variable energizing electric current on the dynamic response characteristics of drilling and hole quality are studied. Experimental results indicate that the vibration frequencies and amplitudes of drilling tool system can be modified by different electric current applied and the surface quality of hole improved effectively. It is demonstrated that the MR fluid damper has the adaptive ability of shifting the response frequency and diminishing the vibration amplitudes of drill head with different control current, and thus a potential targeted suppression of vibrations is obtained.

2. The model of drilling shaft system

[Fig. 1](#) displays the boring trepanning association (BTA) drilling machine. The drilling can be performed with either rotating tool, which is a round hollow drilling shaft tipped with a specially configured drill head, or rotating work-piece, or both if necessary. High pressure cutting fluid injects into the cutting region via the gap between the drilling shaft and hole wall serving as coolant and lubricant at the same time, and flushes the cutting chips from the tool shaft inner hole, which is a kind of the inner ejection deep-hole cutting machining method.

[Deng and Chin \(2004\)](#) firstly established an equation system to describe the drilling tools with pronounced shaft length, and predict the hole roundness by composed of Euler–Bernoulli beam equation. In their formulation, the boundary condition of drilling shaft system is considered as a fixed, simply supported beam, and

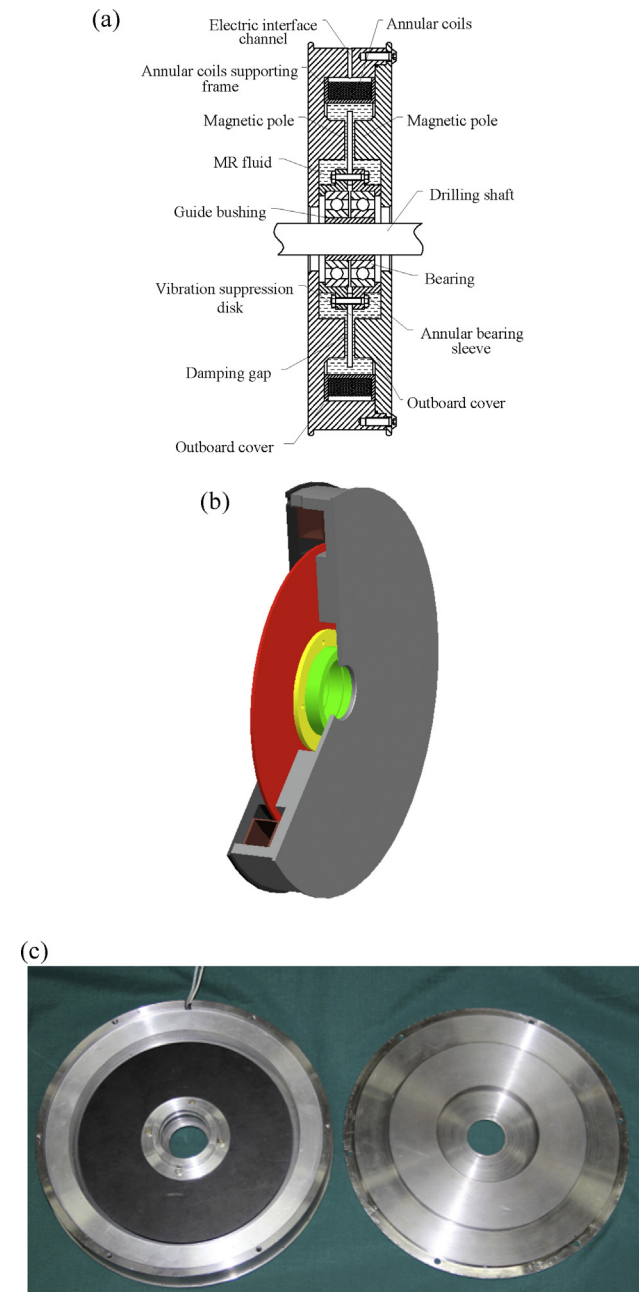


Fig. 2. The design of vibration suppression damper, (a) configuration of vibration suppression damper, (b) 3-D structure of vibration suppression damper and (c) the vibration suppression damper photo.

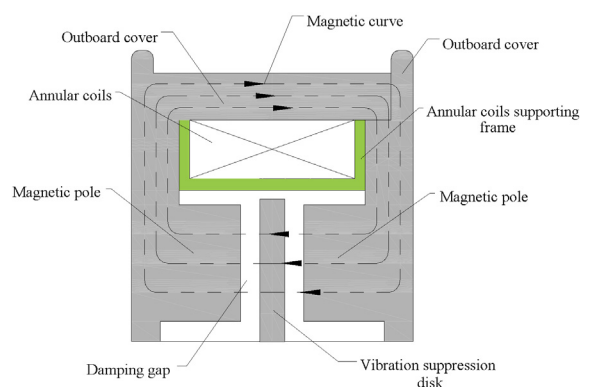


Fig. 3. The magnetic distribution of vibration suppression damper.

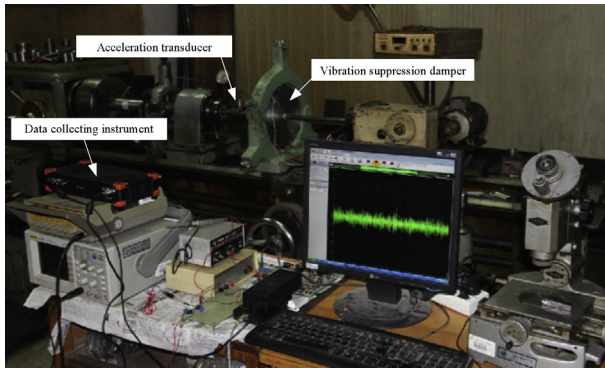


Fig. 4. The experimental arrangement.

thus the governing equation of drilling shaft system can be written as follows:

$$EI \frac{\partial^4(\Delta R)}{\partial z^4} + \rho A \frac{\partial^2(\Delta R)}{\partial t^2} + j2\omega\rho A \frac{\partial(\Delta R)}{\partial t} - \omega^2 \rho A (\Delta R) = f(z, t) \delta(z-l)$$

$$\Delta R = \sqrt{\Delta x^2 + \Delta y^2}$$
(1)

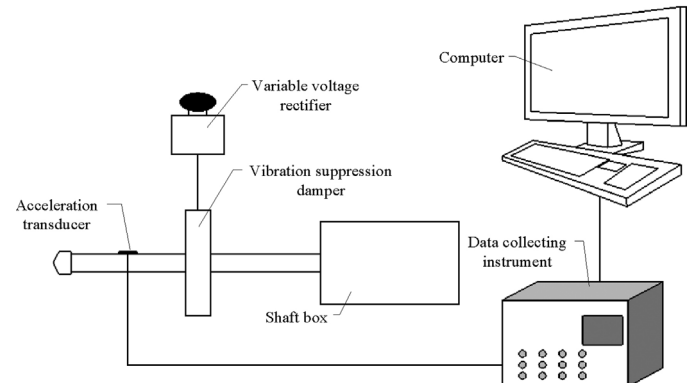


Fig. 5. The scheme of vibration suppression experiment.

where E and I are the Young's modulus and the moments of inertia respectively; ρ is the density of drilling shaft; A is the cross-sectional area of drilling shaft; j is $\sqrt{-1}$; ω is the rotating speed of drilling shaft, and t is time. Additionally, $\delta(z-l)$ is the Dirac-delta function $\delta(z) = \begin{cases} \infty & z = l \\ 0 & \text{otherwise} \end{cases}$, l is the length of drilling shaft; the cutting force $f(z, t)$ is described firstly as a Fourier series by Matin and

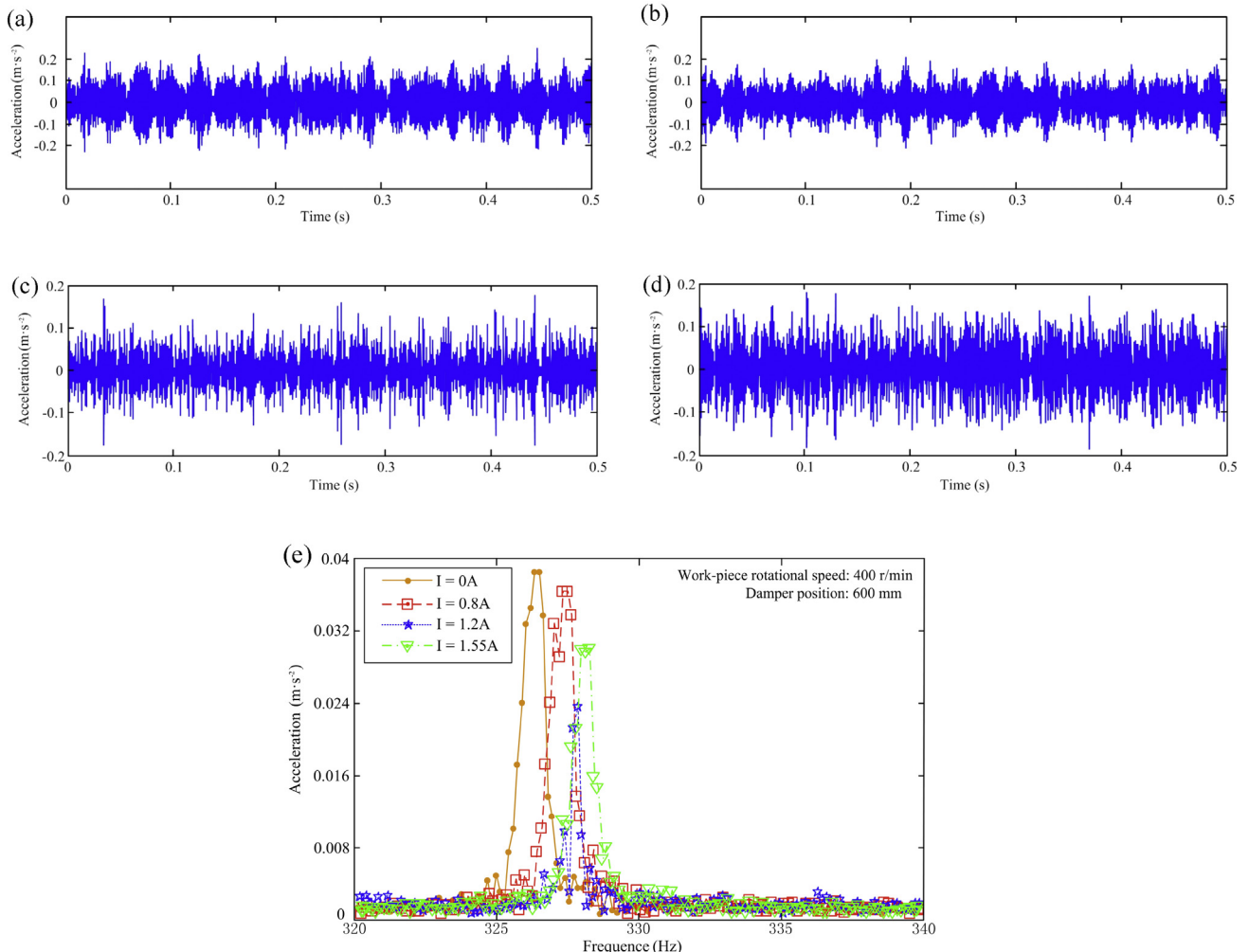


Fig. 6. The vibration responses of drilling shaft at 400 r/min, (a) $I = 0 A$, (b) $I = 0.8 A$, (c) $I = 1.2 A$, (d) $I = 1.55 A$, and (e) the frequency-response curves at different excited electric currents.

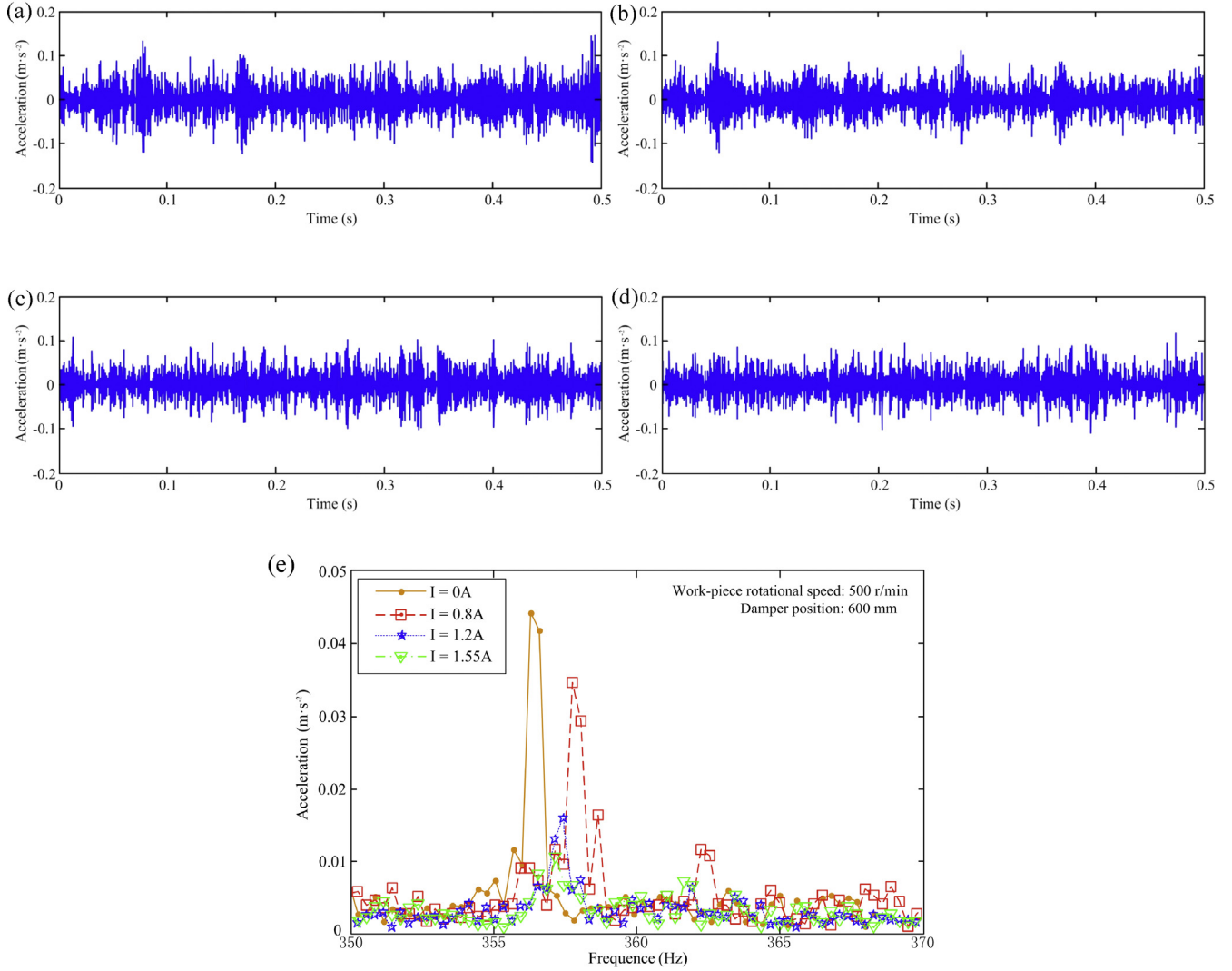


Fig. 7. The vibration responses of drilling shaft at 500 r/min, (a) $I = 0 \text{ A}$, (b) $I = 0.8 \text{ A}$, (c) $I = 1.2 \text{ A}$, (d) $I = 1.55 \text{ A}$, and (e) the frequency–response curves at different excited electric currents.

Rahman (1988), and further, its form is given as (Rahman et al., 1993)

$$f(z, t) = \frac{a_0}{2} + \sum_{m=1}^{\infty} (a_m \cos m\omega t + b_m \sin m\omega t) e^{im\omega(t-z/c_w)} \quad (2)$$

where the coefficients a_0 , a_m and b_m are constant values, and c_w is the wave speed in the work-piece with $c_w = \sqrt{E/\rho}$.

Subsequently, Eq. (1) can be solved by using eigenfunction expansion of $\Delta R(z, t)$, yielding:

$$\Delta R(z, t) = \sum_{i=1}^{\infty} \phi_i(z) q_i(t) \quad (3)$$

where $\phi_i(z)$ and $q_i(t)$ are the mode and modal coordinates of the system, respectively. $\phi_i(z)$ can be expressed by

$$\phi_i(z) = \lambda_1 \cosh(k_n l) + \lambda_2 \sinh(k_n l) + \lambda_3 \cosh(k_n l) + \lambda_4 \sinh(k_n l) \quad (4)$$

where the subscript “ n ” is the mode number, λ_1 , λ_2 , λ_3 and λ_4 are constants, k_n is an undetermined constant of the n th mode. For a fixed, simply supported beam, the beam characteristic $k_n l$ is determined as (Dimarogonas, 1996)

$$\tan(k_n l) = \tanh(k_n l) \quad (5)$$

Substituting Eq. (3) into Eq. (1), the dynamic lateral deflection caused by drilling tool vibration can be obtained as follow:

$$\begin{aligned} \Delta R(z, t) = & \sum_{n=1}^{\infty} \left\{ 2k_n \left[\frac{q_6(t) \cosh(k_n l) \cosh(k_n z)}{2k_n l + \sinh(2k_n l)} \right. \right. \\ & + \frac{q_7(t) \sinh(k_n l) \sinh(k_n z)}{\sinh(2k_n l) - 2k_n l} + \frac{q_6(t) \cos(k_n l) \cos(k_n z)}{2k_n l + \sin(2k_n l)} \\ & \left. \left. + \frac{q_7(t) \sin(k_n l) \sin(k_n z)}{2k_n l - \sin(2k_n l)} \right] \right\} \end{aligned} \quad (6)$$

where $q_6(t)$ and $q_7(t)$ are given by Deng and Chin (2004).

In Eq. (6), it can be seen that the lateral displacement of drilling tool is the summation of many modal effects. In other words, the surface quality of hole in deep hole drilling is directly related to the vibration modes of drill tool that come into existence. This inspires the idea of targeted suppressing, which is simply to knock out the existence of certain harmful vibration mode to neutralize its damage or to force the vibration morph into less harmful modes to curb its damage.

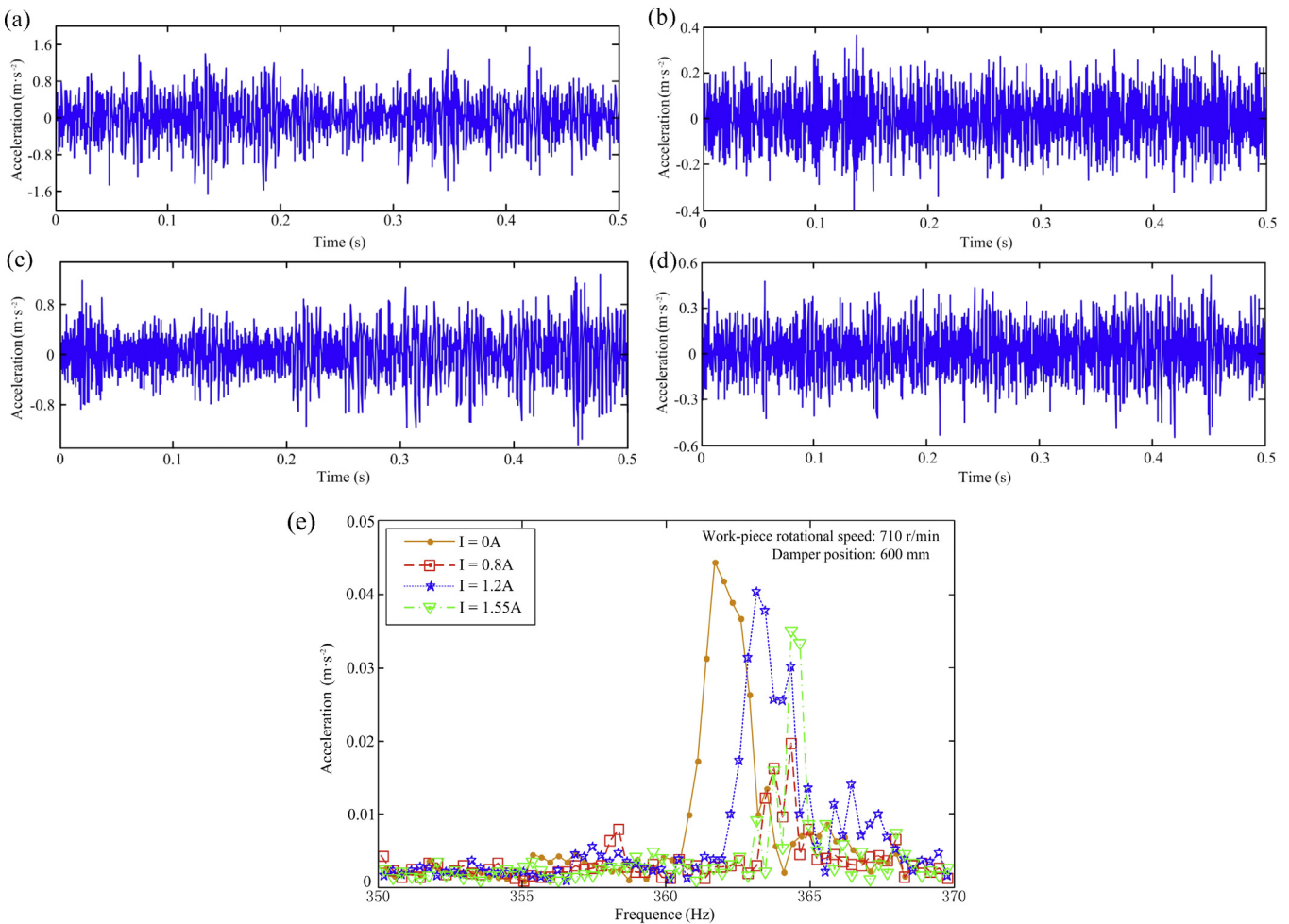


Fig. 8. The vibration responses of drilling shaft at 710 r/min, (a) $I = 0 \text{ A}$, (b) $I = 0.8 \text{ A}$, (c) $I = 1.2 \text{ A}$, (d) $I = 1.55 \text{ A}$ and (e) the frequency–response curves at different excited electric currents.

3. The design and principle of vibration suppression damper

3.1. Design of vibration suppression damper

Fig. 2 shows the designed vibration suppression damper based on shear model, whose main parts are: outboard cover, annular coil, annular coil supporting frame, vibration suppression disk, guide bushing, the ball bearing and annular bearing sleeve. The magneto-rheological (MR) fluid could be injected into the sealed cavity body formed by the annular coils support frame and annular bearing sleeve so as to form the inverter field of solid–liquid conversion. The electrified coils are twined evenly around the inside of annular coil support frame. The number of total coils is 500. The positive and negative terminals of coil are led out through the electric interface channel and connect with the external electric sources. For the vibration suppression damper to have enough magnetic induced strength, a 1 mm gap between the magnetic pole and the vibration suppression disk is necessary. Low-carbon steel material is used for the outboard cover of damper and vibration suppression disk, while aluminum material is used for the annular coil supporting frame and the annular bearing sleeve. Additionally, the Aluminum material has the isolation effect of magnetic field, so all of magnetic curve can be concentrated on magnetic pole along with outboard cover. In this configuration, closed fit between the ball bearing and the guide bushing is adopted, and so the lateral vibration

of drilling shaft in machining process among the drilling shaft, guide bushing and vibration suppression disk are linked together by bolts.

On the other hand, MRF-132DG fabricated by the US Lord company is selected as magneto-rheological fluid. MRF-132DG consists mainly of Hydrocarbon base fluid, and has advantages of little temperature influence, corrosion resistance characteristics, and low viscosity, so as to reduce the structural dimensions of damper and usage amount of MR fluid (Huang et al., 2002). In the meantime, its stress–magnetic strength curve shows a good linearity when the magnetic field is very small, and thus makes the regulation of damping magnitude easily realized in deep hole drilling process.

3.2. Working principle of vibration suppression damper

The working principle of vibration suppression damper with shear mode is as follows: first of all, the operator can select the guide bushing in accordance with the drilling shaft diameter. Since the guide bushing engages the drilling shaft with closed fit, it plays an important role in enhancing the process stability and the hole straightness. The lateral vibration of the drilling shaft transmits through the annular bearing sleeve and lands on the coupled vibration suppression disk where it is counteracted by adjustable damping. The electrical current of annular coils should be regulated in real time based on the conditions of drilling shaft vibration to

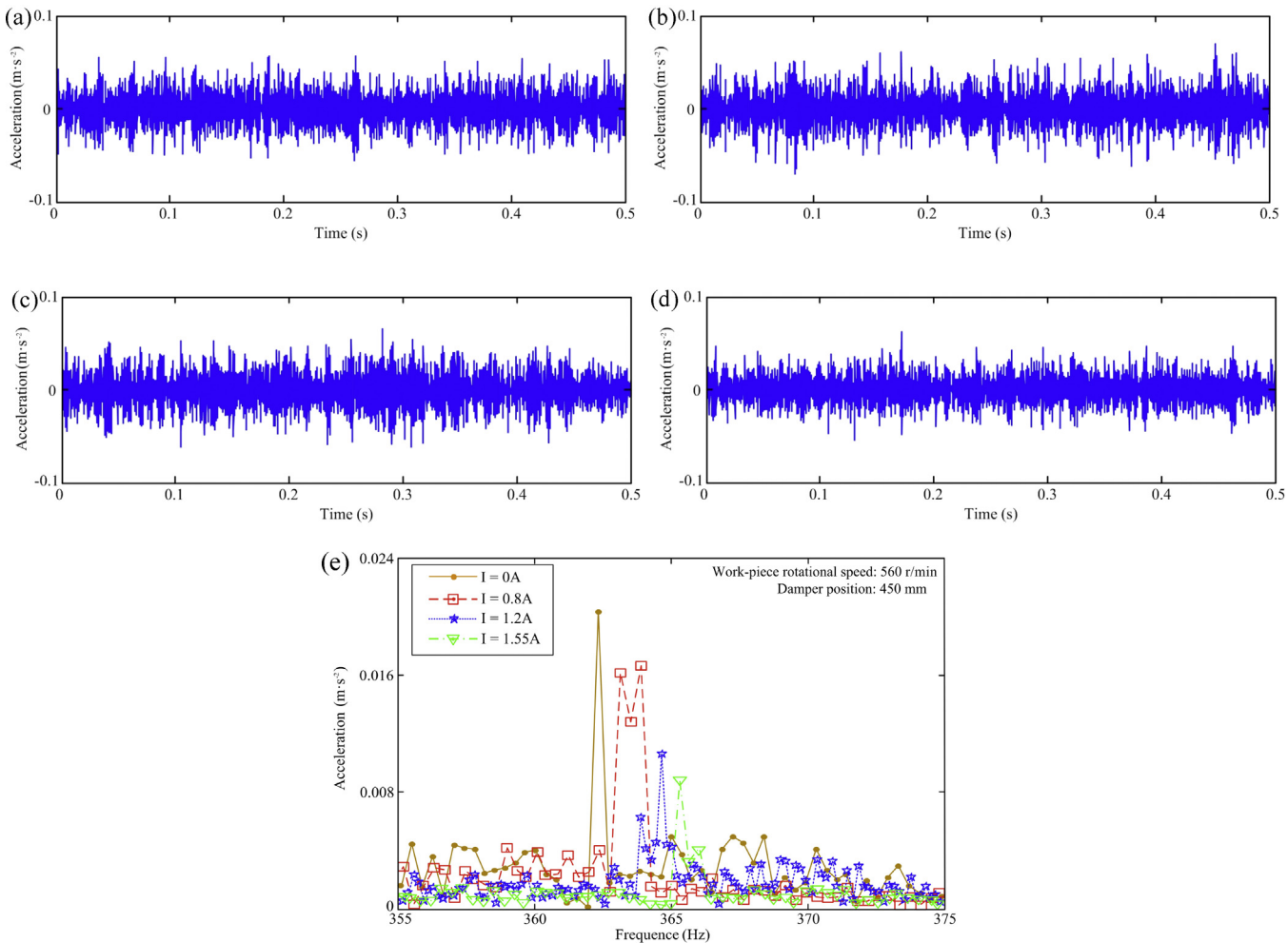


Fig. 9. The vibration responses of drilling shaft at 560 r/min and the installed position of the vibration suppression damper is 450 mm away on the tool head, (a) $I = 0\text{ A}$, (b) $I = 0.8\text{ A}$, (c) $I = 1.2\text{ A}$, (d) $I = 1.55\text{ A}$ and (e) the frequency–response curves at different excited electric currents.

manage the magnetic strengths (the magnetic distribution of vibration suppression damper is indicated in Fig. 3). And then, the MR fluid in the cavity body, energized by the magnetic field, undergoes within nanoseconds a phase conversion between solid and liquid states, whereby changing the shear damping force acting on the disk vibration. For instance, if the drilling shaft vibration worsens during drilling, the appropriately increased electric current in coils enhances magnetic field in the closed cavity body. Accordingly, the MR fluid produces a phase change and become solidified to different degree so as to impede the disk with different shearing damping force. Thus a targeted suppression of vibration is obtained because an actively varied damping responding to the monitored vibration is at hand.

The design suggested in this paper is characterized by the following features: (1) The vibration suppression damper is relatively simple and small, and can be easily installed on various types of deep-hole drilling machines; (2) The MR fluid serves to change the damping value to impede vibrations; (3) This vibration suppression damper not only satisfies the requirement of machine tools with non-rotary workpiece but also satisfies that of machine tools with rotary workpiece as well. Additionally, compared with the design given by Mei et al. (2009), the new design can adapt itself to more widely machining process. Accordingly, it offers better process adaptability.

4. The experiment of vibration suppression

4.1. The scheme of vibration suppression experiment

The experimental rig is set up on a special lathe retrofitted for deep hole drilling with rotary workpiece. The maximum diameter of drilling hole is 30 mm, and the work-piece rotation can be adjusted within the range of 10–1400 r/min. The fixing and supporting of vibration suppression damper are achieved by using the movable intermediate shaft support, as shown in Fig. 4. The correlative parameters are as follows: the drilling shaft is 1.2 m in length, outer diameter of 17 mm and inner diameter 14 mm. Its material is high strength alloy steel, and its density is $7.87 \times 10^3 \text{ kg/m}^3$. Oil supply pressure is $2 \times 10^6 \text{ Pa}$. In order to match easily in the intermediate supports, the outer diameter of vibration suppression damper is 244 mm, and its width is 45 mm. The viscosity of cutting fluid is 0.026 Pa S; the workpiece material is 45# steel. Its length is 400 mm, and drilling depth is 100 mm.

The vibration signals of drilling shaft are collected through the acceleration transducer, which is pre-fixed on the drilling shaft with a distance of 330 mm from the tool head. The data collecting instrument from DEWESOFT company (sampling frequency is 1000 HZ) is used. In the experimental process, the vibration suppression damper is energized with 4 different coil currents of 0 A,

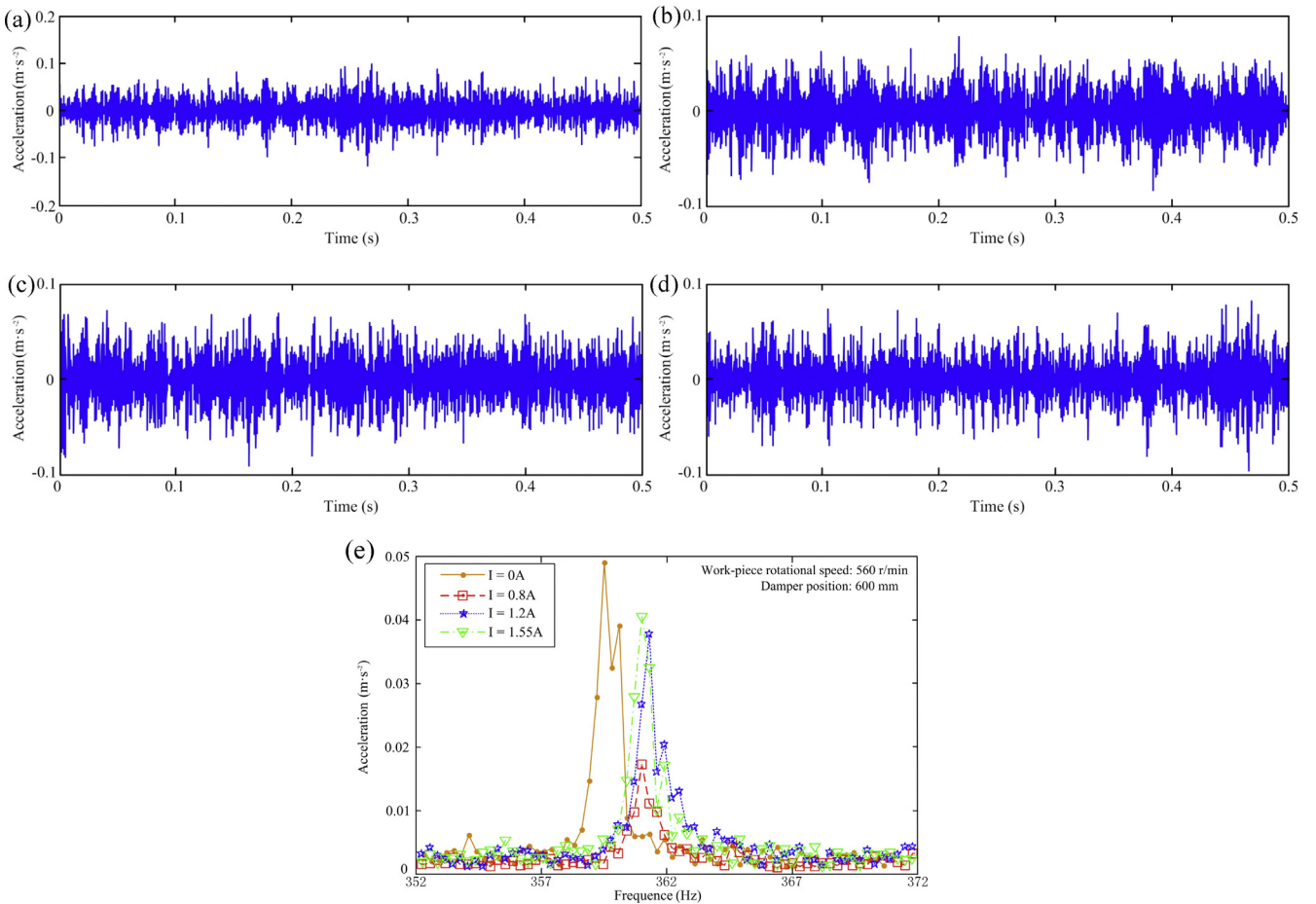


Fig. 10. The vibration responses of drilling shaft at 560 r/min and the installed position of the vibration suppression damper is 600 mm away on the tool head, (a) $I=0\text{ A}$, (b) $I=0.8\text{ A}$, (c) $I=1.2\text{ A}$, (d) $I=1.55\text{ A}$ and (e) the frequency-response curves at different excited electric currents.

0.8 A, 1.2 A and 1.55 A respectively, and the feed rate of tools is 0.024 mm/r. Based on the vibration characteristic of drilling shaft, the annular coils current is changed via the variable voltage rectifier to produce the inner magnetic field, whereby controlling over the damping values of vibration suppression disk. And then, the vibration signals in the drilling process are obtained via the signal collector and computer, and the corresponding data processing is conducted with the help of DEWSOFT spectral analysis software. The scheme of the experiments is shown in Fig. 5.

4.2. The results and discussion of vibration suppression experiment

4.2.1. The suppression effects of drilling shaft under different work-piece rotation speeds

In order to evaluate the effectiveness of the design, the lateral vibration signals of drilling shaft and the machined hole surfaces are analyzed. Figs. 6–8 show the experimental results of shaft vibration upon actuation of vibration suppression. The work-piece rotates at 400, 500 and 710 r/min respectively and the MR damper exerts on the tool shaft at a position of 600 mm away from the tool head.

It is seen from Figs. 6–8 that for each rotational speed, frequency responses of the drilling shaft are modulated in magnitude and frequency, and both downsize effect in magnitude and shift effect in frequency are obvious. These results are very encouraging in that a targeted suppression of vibration and a shift away from dangerous frequency is possible. Suppression effects appear different for different rotation speed. For instance, for 710 r/m in Fig. 8, the

best suppression effect is obtained with $I=0.8\text{ A}$, producing an amplitude reduction of 60%, which also corresponds to the smallest hole surface roughness $R_a = 1.75 \mu\text{m}$ in Table 1. For 400 r/min in Fig. 6, the suppression effects are moderate. Nevertheless, there exists an optimal control current $I=1.2\text{ A}$ while stronger current 1.5 A does not bring better suppression effect. In addition, it can be seen from Figs. 6–8 that there exists a large difference in the frequency shift effect. In 710 r/min the frequency shift effect is much bigger, with resonant frequency raised from 361.6 Hz when $I=0\text{ A}$ –364.4 Hz when $I=1.55\text{ A}$. Experience from Mehrabadi et al. (2009) showed that the frequency shift effect of vibration suppression can effectively improve the stability of drilling tools. Dilley et al. (2005) observed a frequency shift which they attributed to margin engagement and pointed out that its gradual development poses a potential matching of some unwelcome frequencies in process, however, contrary to the inevitable margin-engagement initiated one, the current initiated frequency shift could be used to “jump” off from harmful frequency match during drilling.

4.2.2. The suppression effects of drilling shaft under different suppression positions

The location of damper is another factor in vibration suppression. It is conceivable that a midspan location would force the first mode vibration into second mode, etc. But at this stage only the effectiveness of the MR damper is evaluated. Figs. 9–11 show the responses of a drill shaft rotating at 560 r/min and suppressed by the MR damper mounted at a distance of 450 mm, 600 mm and 750 mm from tool head respectively. It is seen from Figs. 9–11 that

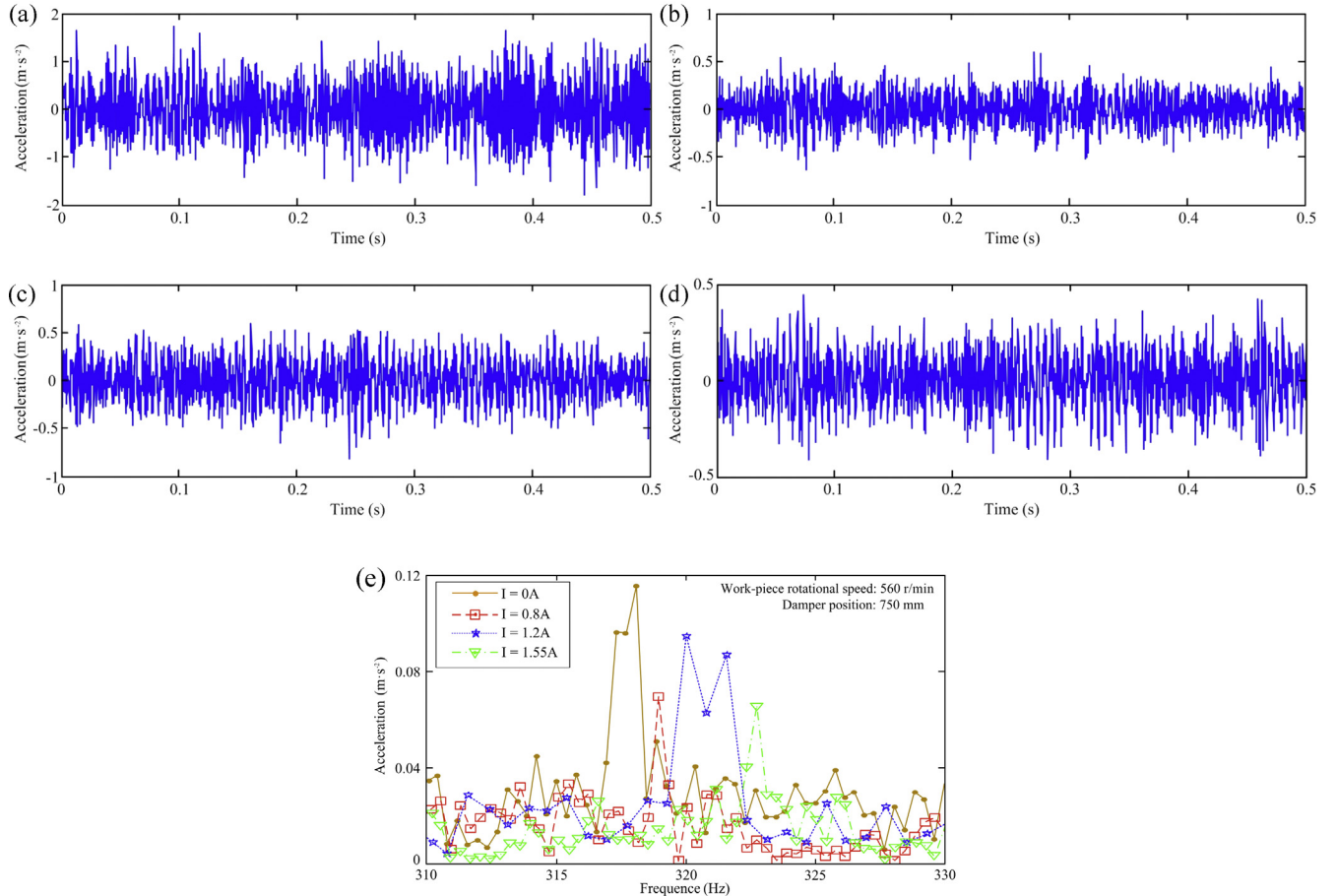


Fig. 11. The vibration responses of drilling shaft at 560 r/min and the installed position of the vibration suppression damper is 750 mm away on the tool head, (a) $I = 0 \text{ A}$, (b) $I = 0.8 \text{ A}$, (c) $I = 1.2 \text{ A}$, (d) $I = 1.55 \text{ A}$ and (e) the frequency-response curves at different excited electric currents.

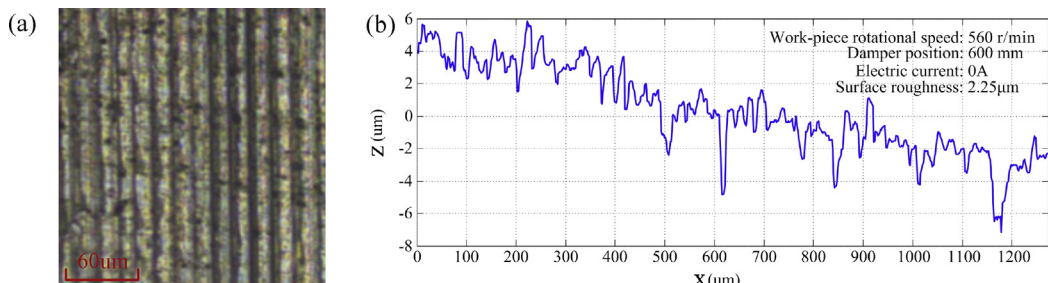


Fig. 12. The machined surface picture and the surface roughness of workpiece with MR damper control (the electric current $I = 0 \text{ A}$ and rotational speed 560 r/min), (a) the picture of machined surface and (b) the curve of surface roughness ($R_a = 2.25 \mu\text{m}$).

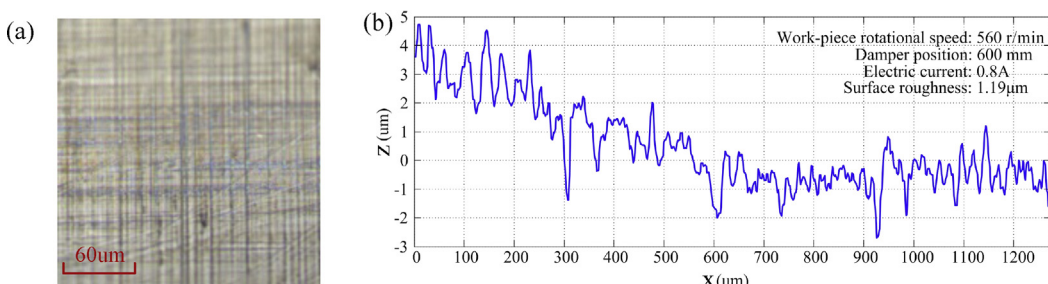


Fig. 13. The machined surface picture and the surface roughness of workpiece with MR damper control (the electric current $I = 0.8 \text{ A}$ and rotational speed 560 r/min), (a) the picture of machined surface and (b) the curve of surface roughness ($R_a = 1.19 \mu\text{m}$).

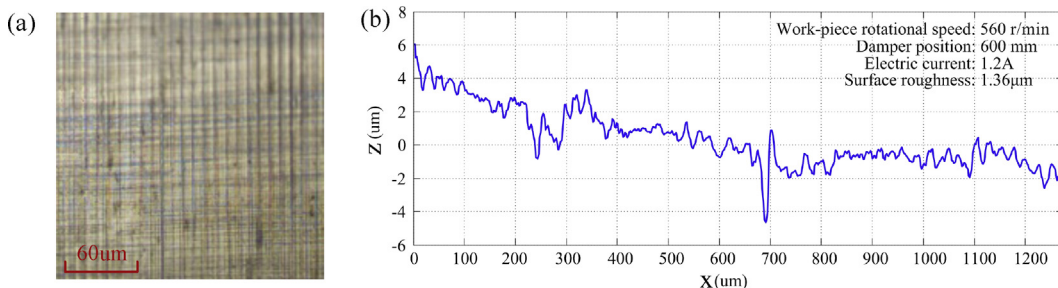


Fig. 14. The machined surface picture and the surface roughness of workpiece with MR damper control (the electric current $I = 1.2$ A and rotational speed 560 r/min), (a) the picture of machined surface and (b) the curve of surface roughness ($R_a = 1.36$ μm).

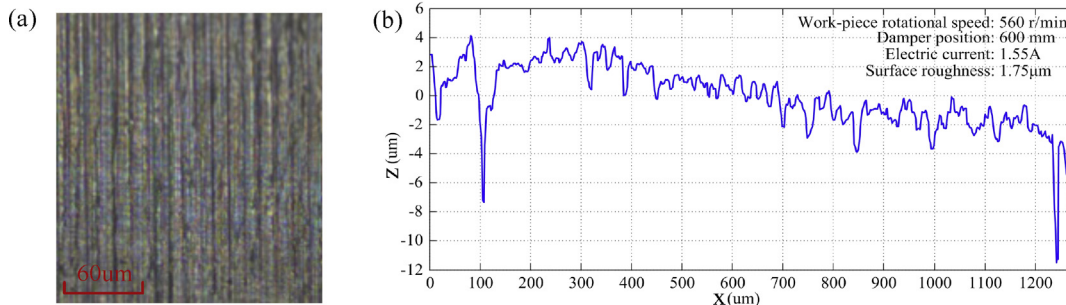


Fig. 15. The machined surface picture and the surface roughness of workpiece with MR damper control (the electric current $I = 1.55$ A and rotational speed 560 r/min), (a) the picture of machined surface and (b) the curve of surface roughness ($R_a = 1.75$ μm).

the position of the vibration suppression damper has an obvious effect on the lateral vibration of shaft system. Once the position of vibration suppression is changed, the results of suppression change accordingly and there exists a different appropriate exciting electric current. The main reason is that the drilling shaft system with one or more intermediate support is typically a multi-body continuum in machining process. Although cutting forces and intermediate shaft support act locally, the effects from them are global and coupled with each other (Deng et al., 2001). In addition, the energy storage modulus and energy consumption modulus of magneto-rheological fluid are not only subject to the magnetic field, but also manifest strong nonlinearity in its mechanism (Bellan and Bossis, 2002). On the other hand, the testing results in Figs. 9–11 indicate that there exists an appropriate energizing electric current for each kind of workpiece rotational speed or a position of the vibration suppression damper.

4.2.3. The hole surface under different suppression conditions

In the actual deep hole drilling process, the biggest concern is the quality of hole surface. The experimental values of machined hole surface roughness obtained under different conditions of different workpiece revolution speeds or the vibration suppression positions respectively are listed in Table 1 (The roughness measuring instrument is produced by LEICA DCM3D). From Table 1, it can be seen that under the same machining conditions, surface

roughness has been improved in all cases of vibration suppression with difference in the applied current intensity. A very interesting question arises from Table 1: does the smallest roughness always correspond to the optimal suppression current? Take 500 r/min as an example, the smallest $R_a = 1.47$ is obtained with $I = 1.2$ A, but a check with Fig. 7 reveals that the optimal suppression current is $I = 1.55$ A which produces the second best $R_a = 1.53$ in Table 1. An extra month of experiments reveals that an additional parameter, the wear on the cutting edge, participates in the producing of roughness and is particularly pronounced when the vibration suppression effects by the different coil currents reach similar magnitude. Since wear observation is out of the scope of this study, the assumable point that the best suppression produces the smallest R_a is temporarily not claimed in this study. The vibration suppression principle suggested and implemented in this paper has been proven effective to improving the hole machining qualities. For instance, if the workpiece rotational speed is selected as 560 r/min, the vibration suppression damper is installed 600 mm away from the tool head, and the excited electric current is selected as 0.8 A, the optimum deep-hole surface roughness of 1.19 μm can be obtained. Additionally, Figs. 12–15 show the picture of the machined surface with vibration suppression damper control. Not only did the chatter marks decrease clearly, but the surface roughness also decreased from 2.25 μm to 1.19 μm R_a when the different excited electric currents were activated.

Table 1

The influence of the MR fluid vibration damper on the surface roughness of hole (R_a).

The excited electric current	Work-piece revolution speeds (The MR damper mounted at a distance of 600 mm from tool head)			The vibration suppression positions (The work-piece rotates at 560 r/min)		
	400 r/min	500 r/min	710 r/min	450 mm	600 mm	750 mm
0 A	$R_a = 2.26$ μm	$R_a = 2.31$ μm	$R_a = 2.53$ μm	$R_a = 1.91$ μm	$R_a = 2.25$ μm	$R_a = 2.83$ μm
0.8 A	$R_a = 1.95$ μm	$R_a = 2.11$ μm	$R_a = 1.75$ μm	$R_a = 1.88$ μm	$R_a = 1.19$ μm	$R_a = 2.59$ μm
1.2 A	$R_a = 1.63$ μm	$R_a = 1.47$ μm	$R_a = 2.33$ μm	$R_a = 1.86$ μm	$R_a = 1.36$ μm	$R_a = 2.77$ μm
1.55 A	$R_a = 2.09$ μm	$R_a = 1.53$ μm	$R_a = 2.16$ μm	$R_a = 1.75$ μm	$R_a = 1.75$ μm	$R_a = 2.42$ μm

5. Conclusions

- (1) This paper proposes a concept of precision or targeted suppression of tool vibration in deep hole drilling. A vibration suppression damper using magneto-rheological fluid is designed and fabricated.
- (2) The construction of the vibration suppression damper is relatively simple and small. It can be used in the drilling process of tool rotating or workpiece rotating.
- (3) Under the action of different applied electric current, the vibration suppression damper is able to suppress the tool vibration significantly and with accompanied frequency shift whereby effectively improves the surface quality of machined holes.
- (4) Different suppression location generates different suppression results. Therefore the combination of suppression location and suppression strength offers a broader base in vibration suppression.
- (5) A precision or targeted suppression of long shaft vibration appears feasible if comprehensive experiments are performed.

In future study, comprehensive experiments and theoretical analysis will be performed to clarify the deterministic effects of different suppression location on the vibration, and to accumulate more knowledge for targeted suppression of vibration for deep hole drilling based on at least the suppression location and strength. Wear on drilling edge will also be observed to check the validity of the assumption that the best suppression also always produces the least roughness.

Acknowledgments

This work is supported by National Natural Science Foundation of China (Grant Nos. 51105305 and 51275407), National Science and Technology Major Project of the Ministry of Science and Technology of China (Grant Nos. 2013ZX0400901 and 2012ZX04012-032), the Major Research Program of Shaanxi Province of China (13115 Project, Grant No. 2009ZDKG-25), and

Natural Science Foundation of Department of Education of Shaanxi Province of China (No. 12JK680).

References

- Bayly, P.V., Lamar, M., Calvert, S., 2002. Low-frequency regenerative vibration and the formation of lobed holes in drilling stability of interrupted cutting by temporal finite element analysis. *ASME J. Manuf. Sci. Eng.* 124, 275–285.
- Bellan, C., Bossis, G., 2002. Field dependence of viscoelastic properties of MR elastomers. *Int. J. Mod. Phys. B* 16, 2447–2453.
- Deng, C.S., Chin, J.H., 2004. Roundness errors in BTA drilling and a model of waviness and lobing caused by resonant forced vibrations of its long drill shaft. *ASME J. Manuf. Sci. Eng.* 126, 524–534.
- Deng, C.S., Huang, J.C., Chin, J.H., 2001. Effect of support misalignment in deep-hole drill shafts on hole straightness. *Int. J. Mach. Tools Manuf.* 41, 1165–1188.
- Dilley, D.H., Stephenson, D.A., Bayly, P.V., Schaut, A.J., 2005. Frequency shift in drilling due to margin engagement. *ASME J. Manuf. Sci. Eng.* 127, 271–276.
- Dimarogonas, A., 1996. *Vibration for Engineering*, 2nd ed. Prentice Hall International Editions, New Jersey.
- Gessesse, Y.B., Latinovic, V.N., Osman, M.O.M., 1994. On the problem of spiraling in BTA deep-hole machining. *J. Eng. Ind.* 116, 161–165.
- Huang, J., Zhang, J.Q., Yang, Y., Wei, Y.Q., 2002. Analysis and design of a cylindrical magneto-rheological fluid brake. *J. Mater. Process. Technol.* 129, 559–562.
- Hussien, M.A.W., Rama, B.B., Kudret, D., 2007. Whirling vibration in boring trepanning association deep hole boring process: analytical and experimental investigations. *ASME J. Manuf. Sci. Eng.* 129, 48–62.
- Keraita, J., Oyango, H., Misoi, G., 2001. Lathe stability charts via acoustic emission monitoring. *Afr. J. Environ. Sci. Technol.* 2, 81–93.
- Litak, G., 2002. Chaotic vibrations in a regenerative cutting process. *Chaos Soliton Fract.* 13, 1531–1535.
- Matin, M.A., Rahman, M., 1988. Analysis of the cutting process of a cylindrical work-piece clamped by a three-jaw chuck. *J. Eng. Ind.* 110, 326–332.
- Mehrabadi, I.M., Nouri, M., Madoliat, R., 2009. Investigating chatter vibration in deep drilling, including process damping and the gyroscopic effect. *Int. J. Mach. Tools Manuf.* 49, 939–946.
- Mei, D.Q., Kong, T.R., Shih, A.J., Chen, Z.C., 2009. Magnetorheological fluid-controlled boring bar for chatter suppression. *J. Mater. Process. Technol.* 209, 1861–1870.
- Messaoud, A., Weihua, C., 2009. Monitoring a deep hole drilling process by nonlinear time series modeling. *J. Sound Vib.* 321, 620–630.
- Rahman, M., Matin, M.A., Seah, K.H.W., 1993. A Study of the vibrational dynamics of an endmill clamped by side-locking. *J. Eng. Ind.* 115, 438–443.
- Weinert, K., Webber, O., Hüskens, M., Mehnert, J., Theis, W., 2002. Analysis and prediction of dynamic disturbances of the BTA deep hole drilling process. In: *Proceedings of the Third CIRP International Seminar on Intelligent Computation in Manufacturing Engineering*, pp. 297–302.
- Yao, Z.H., Mei, D.Q., Chen, Z.C., 2011. On-line chatter detection and identification based on wavelet and supportvector machine. *J. Mater. Process. Technol.* 210, 713–719.